Available online at www.sciencedirect.com
SCIENCE DIRECT®
Journal of Power Sources 115 (2003) 131–136
JOURNAL OF POWER SOURCES
www.elsevier.com/locate/jpowsour

Thermal analysis and modeling of a notebook computer battery

Hossein Maleki*, Ahmad K. Shamsuri
Motorola Energy System, 1750 Bell Meade Court, Lawrenceville, GA 30045, USA

Received 20 November 2002; accepted 28 November 2002

Abstract

Thermal performance of an intelligent notebook computer battery-pack (IBA2+™, Hewlett Packard) was evaluated during operation at 42 °C using a combination of thermal analysis and modeling. The battery-pack was charged at 2.36 A and provided 55-W constant power during discharge. Results showed the battery-pack has reasonable heat dissipation capability except that the temperature rise of its charge control IC increases to 67 °C, which is near the critical thermal limit of the device (73–75 °C). Autopsy results showed this IC has a small die to die-pad size ratio and also large volume of mold compound causing the device self-heating during the charge control process. Thermal modeling provided a detailed understanding of the thermal response of the battery under various operating conditions that helped to reduce the product design cycle-time. The overall results indicated that the battery temperature rise during charge is dominated by the power dissipation from the control electronics and during discharge by the heat dissipation from Li-ion cells.

Keywords: Li-ion cells; Thermal modeling; Computer battery packs

1. Introduction

Demands for high power and compact portable electronics products (e.g. cell-phones and laptop computers) are growing daily. Rechargeable Li-ion cells have become the power source of choice for most portable electronic products, because of their high power density, long cycle-life and practical range of operating voltage (2.8–4.2 V). Today's cylindrical 18650 Li-ion cells provide 485 Wh/l. Application of Li-ion cells has been limited because of their self-heating under moderate to high levels of discharging currents (>*C*-rate) and operation at or exposure to temperatures above 60 °C. Li-ion cells generate significantly higher heat during discharge than during charge. For safety reasons, cylindrical Li-ion cells are often equipped with current interrupt devices, shutdown separators and vent mechanisms. These devices, however are not particularly effective after initiation of thermal runaway in Li-ion cells.

Therefore, Li-ion batteries rely on electronic controls to protect them against overcharge, overdischarge and short circuits. For batteries, design of a reliable safety architecture is complex and also depends on the type of product and its application requirements. Application of two to three levels of safety protection for overcharge, over/under currents and electrical hard/soft short circuits in computer batteries are commonly used.

Intelligent Battery Architecture (IBA™) is one of the design platforms employed by Hewlett Packard for their notebook battery power management design. IBA2+ is the latest generation of IBA design platform and provides cost and flexibility advantages in controlling multiple battery configurations. One of the distinct design features of this battery is its internal charge converter that employs integrated charge control ICs capable of leveling cell voltages during charge. Special efforts are made to ensure that the temperature rise of the converter, due to self-heating, stays below its recommended limit (75 °C) and also that it does not cause the temperature of the neighboring components to rise above their critical limits.

This article deals with prediction of thermal response of the control electronics and Li-ion cells in an IBA2+ battery during discharge/charge. Computational Fluid Dynamic software (Ice-Pak, Fluent Inc., USA) was used for thermal modeling. Experimental data in support of the modeling results are also included.

2. Thermal modeling

The battery thermal models are based on the heat generation of Li-ion cells and control electronics during charge/

* Corresponding author. Tel.: +1-770-338-3146; fax: +1-770-338-3321.
E-mail address: g14451@motorola.com (H. Maleki).

0378-7753/03/$ – see front matter © 2003 Elsevier Science B.V. All rights reserved.
doi:10.1016/S0378-7753(02)00722-X

discharge. For modeling simplification, architectures of some of the electronic components (e.g. capacitors and inductors) were modeled as lumped systems. The critical components such as the charge control ICs, FETs and diodes detailed architecture (die, pad, leads, and wire-bonds) and also the geometries of the PCB were used to create the models.

2.1. Li-ion cells

The cell total heat generations during discharge/charge was determined using the following relation:

$$\dot{Q} = I(V_{ocv} - V_{op}) - I\left(T\frac{dV_{ocv}}{dT}\right) \quad (1)$$

where $\dot{Q}$ is the total heat generation from the cell, I the discharge current (A), V_{ocv} the open circuit voltage (V), V_{op} the operating voltage (V), and T is the temperature (K).

In Eq. (1), the $I(V_{ocv} - V_{op})$ term is the "irreversible" heat generation that results from the IR drop and polarization impedances in Li-ion cells; and $IT(dV/dT)$ is the heat generation from thermodynamic effects that is also called "reversible" heat. The reversible heat is generally smaller than the irreversible heat by a factor of 3–4 depending on the current rate and the type of active materials used in the Li-ion cells. Methods for obtaining the heat generation profile of Li-ion cells during charge/discharge are given elsewhere [1]. Fig. 1 compares irreversible heat generation profiles of a single 2.0 Ah 18650 Li-ion cell versus multi-cell units connected in parallel (P) and/or series (S): 2P, 2S, 2P × 2S and 2P × 4S. The cells were discharged at 45 °C ambient while providing power values in multiples of 6.25 W: a single cell provided 6.25 W; 2P and 2S cells, 12.5 W; 2P × 2S cells, 25 W; and 2P × 4S cells, 50 W.

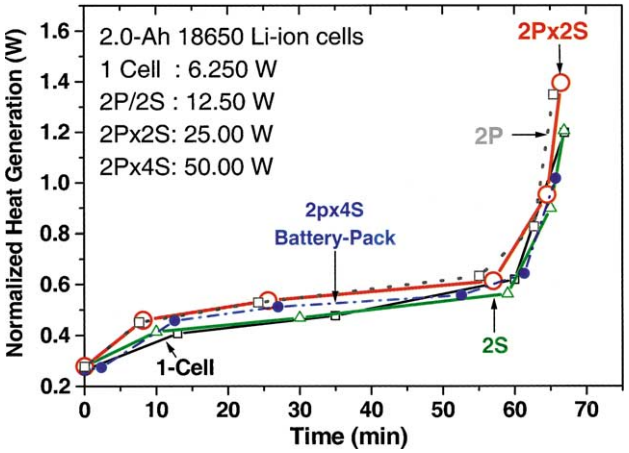

Fig. 1. Heat generation profiles of 2.0 Ah 18650 Li-ion single cell vs. cells connected in parallel (P) and/or series (S). Heat profiles of the multi-cell units are normalized to number of cells in given assembly.

In Fig. 1, the heat generation profile of each multi-cell unit is "normalized" to the number of cells in its assembly. Note that the heat generation profile of a Li-ion cell is nearly the same regardless of its assembling configuration. This result shows that the measured heat generation from one cell can be assigned to any cell in the battery-pack, regardless of its arrangement (in parallel and/or series). Such an approach

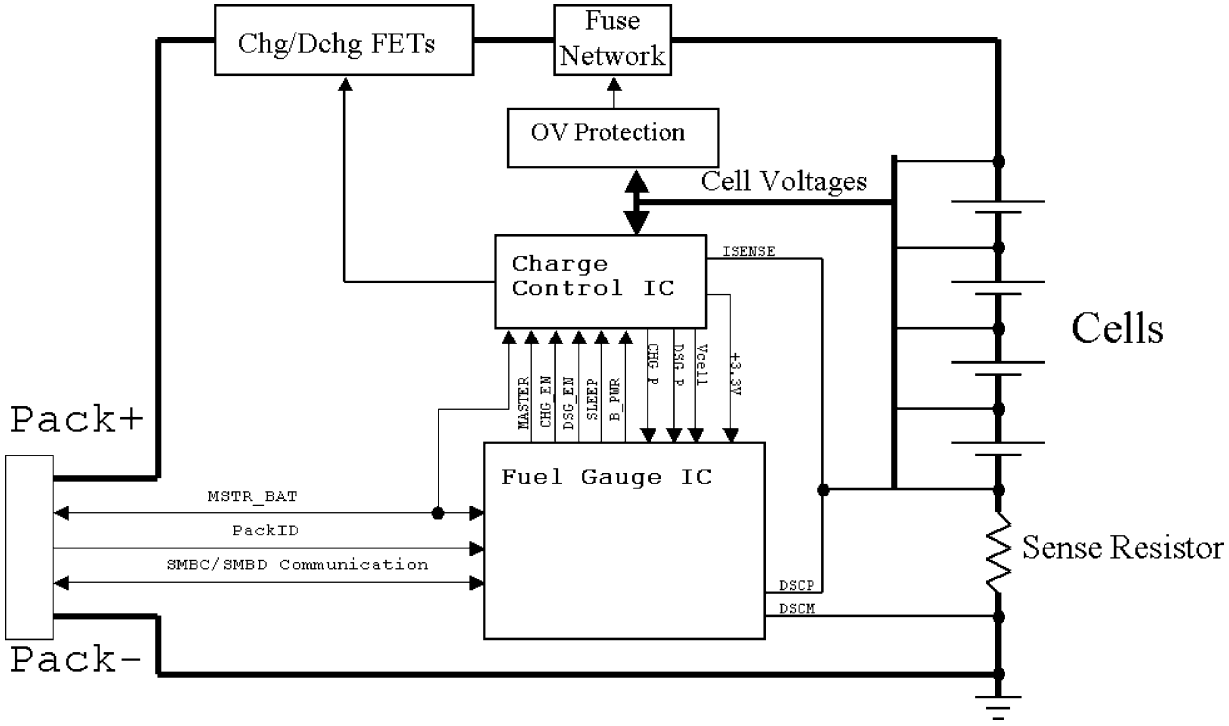

Fig. 2. Block diagrams of the control electronics of the IBA2+ battery.

Table. 1
Properties of common materials used in electronic components and PCBs

Components internal parts	Density (kg/m^3)	Heat capacity (J/kg K)	Thermal conductivity (W/m.K)
Die	2330	711	100
Die attached/glow	4000	770	265
Mold compound	2000	840	0.7
Copper	89000	380	386
Solder	8420	176	50
FR4/PCB	2000	840	0.35
Lead/dap	8900	380	386

allows building thermal models of a battery-pack, with multiple cells, simply by measuring the heat generation profile of one cell rather than first building a battery-pack and then measuring its overall heat generation. Using this single cell heat generation data in modeling greatly reduces both modeling and design cycle-time without compromising accuracy.

2.2. Electronic components

Significant modeling detail is often necessary for accurate thermal simulation of electronic components (e.g. power ICs). For full system-level modeling such as battery-packs, it is not practical to model all electronic components to the degree of detail used in single-device simulations. Detailed information on simplification of full-scale products is given elsewhere [2,3]. Fig. 2 shows block diagrams of the control electronics of the IBA2+ battery.

Table 1 gives properties of typical materials used in the electronic components. This data was used to calculate effective density (ρ), heat capacity (C_p) and thermal conductivity (K) of the electronics components in the IBA2+ battery.

For the lumped electronics parts (capacitors and inductor), the associated leads on each side of a device are lumped to one block having the same physical properties and contact areas to the PCB as all the leads combined. The effective properties for each device are determined using the following relations.

$$\text{Density}\ (\rho) = \frac{\sum(\rho V)_i}{\sum V_t}.$$

$$\text{Heat capacity}\ (C_p) = \frac{\sum(C_p V)_i}{\sum V_t}.$$

$$\text{Thermal conductivity}\ (K) = \frac{\sum(KV)_i}{\sum V_t}.$$

Soldering (Pb 39.2% : Sn 60.8%) thickness was 60 μm.

2.3. Printed circuit board (PCB)

PCBs are made of multiple layers of thin copper foils and a dielectric material (FR4) with many thermal and electrical vias. Because of the copper layers, PCBs have a significantly higher thermal conductivity along the in-plane direction than in the through-plane. Therefore, calculation of correct thermal properties is critical and does influence device heating or cooling rates, as well as the overall thermal performance of the host product. An orthotropic thermal conductivity must therefore be applied in order to account for the differences between thermal conductivity of in-plane versus through-plane direction. The AT&T model can be used to calculate the effective in-plane and through-plane thermal conductivity for PCBs [4]. However, we have used the Ice-Pak simulation package that allows calculation of the density, heat capacity and thermal conductivity of PBCs based on their layout design including the FR4 geometry and number, thickness and percentages of copper layers.

Table 2 lists the power dissipation values for the IBA2+ battery critical components during discharge and charge. The values were calculated based on the currents needed to provide 55-W constant power during discharge and current to charge the battery-pack to full level in about 2 h. The

Table 2
Heat generation and temperature rise of the electronic components and cells in battery-pack during discharge and charge

Electronic components	Components heat generation (W)		Temperature rise (°C)			
	Discharge	Charge	End of the discharge (12.0 V)		End of the charge (16.8 V)	
			Experimental	Model	Experimental	Model
Capacitor	0.0	0.0829	66	64–66	65	58–61
Cells	Based on profile	Based on profile	60	62–70	52	45–51
Charge control IC	0.0042	0.5	66	64–67	71	58–67
Diode-B, D2	Off	0.0	65	65–68	67	60–61
Diode-F, D1	0.0	0.0451	65	65–66	66	58–61
Fuel gauge	0.000825	0.000825	63	64–66	62	59
Charge FET	0.00475	0.4639	65	66–68	72	65–69
Discharge FET	0.1447	0.0501	71	66–67	66	59–62
Bypass discharge FET	0.1102	0.0	66	66–67	66	60–61
Sense resistor	0.3216	0.1113	87	76–83	64	58–61
Inductor	0.009	0.4103	66	64–68	68	60–63

current during discharge was 4.0 A, and 2.36 A during charge as the maximum limit was set by the charge control IC. Heat generation from electronics and cells were used to simulate the battery-pack thermal response for the given sets of condition noted above.

3. Modeling steps

1. Measured the reversible/irreversible heat generation from a 2.2-Ah Li-ion cell (Toshiba 18650U) during discharge and charge.

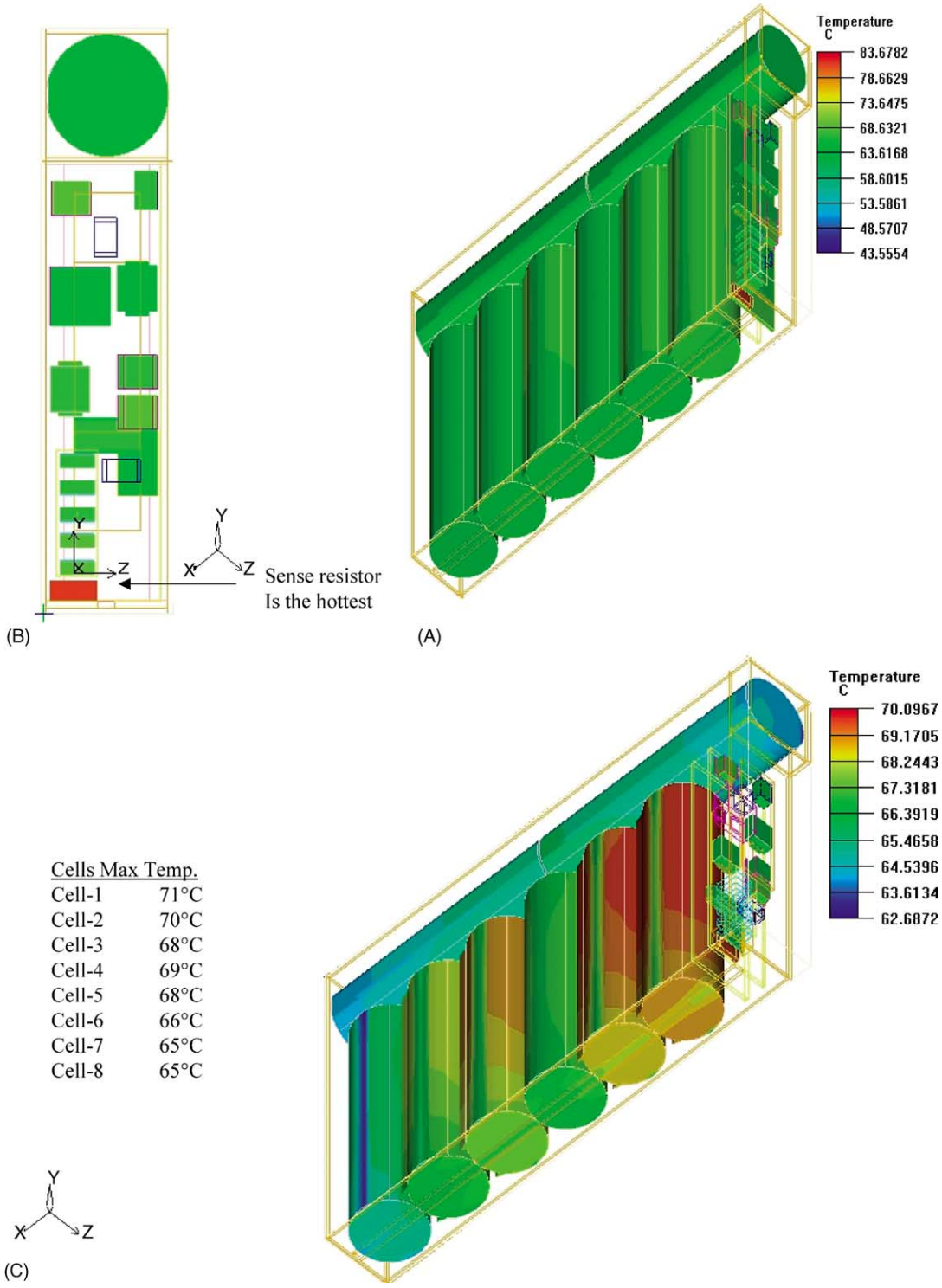

Fig. 3. (A) Global thermal profiles of the IBA2+ battery at the end of the discharge state. (B) Global thermal profile of the power board in the IBA2+ battery. (C) Thermal profiles of the IBA2+ battery at the end of the discharge state. Temperature profile is focused between 62 and 71 °C for higher resolution.

2. Assign the heat generation from item-1 to each of the eight cells in the battery-pack.
3. Density, heat capacity and thermal conductivity of the cells are calculated using the experimental data and methodology described in [5].
4. Treated each cell as a cylindrical solid-block that generated heat during a discharge and charge cycle.
5. The inductor, capacitors and sense resistor are lumped; the charge and discharge control ICs, FETs and Diodes are molded in details because of the importance of their role in thermal performance of the battery-pack.
6. All control electronics generate constant heat during operation depending on their functionality in the battery operation. Device heat generation values are calculated

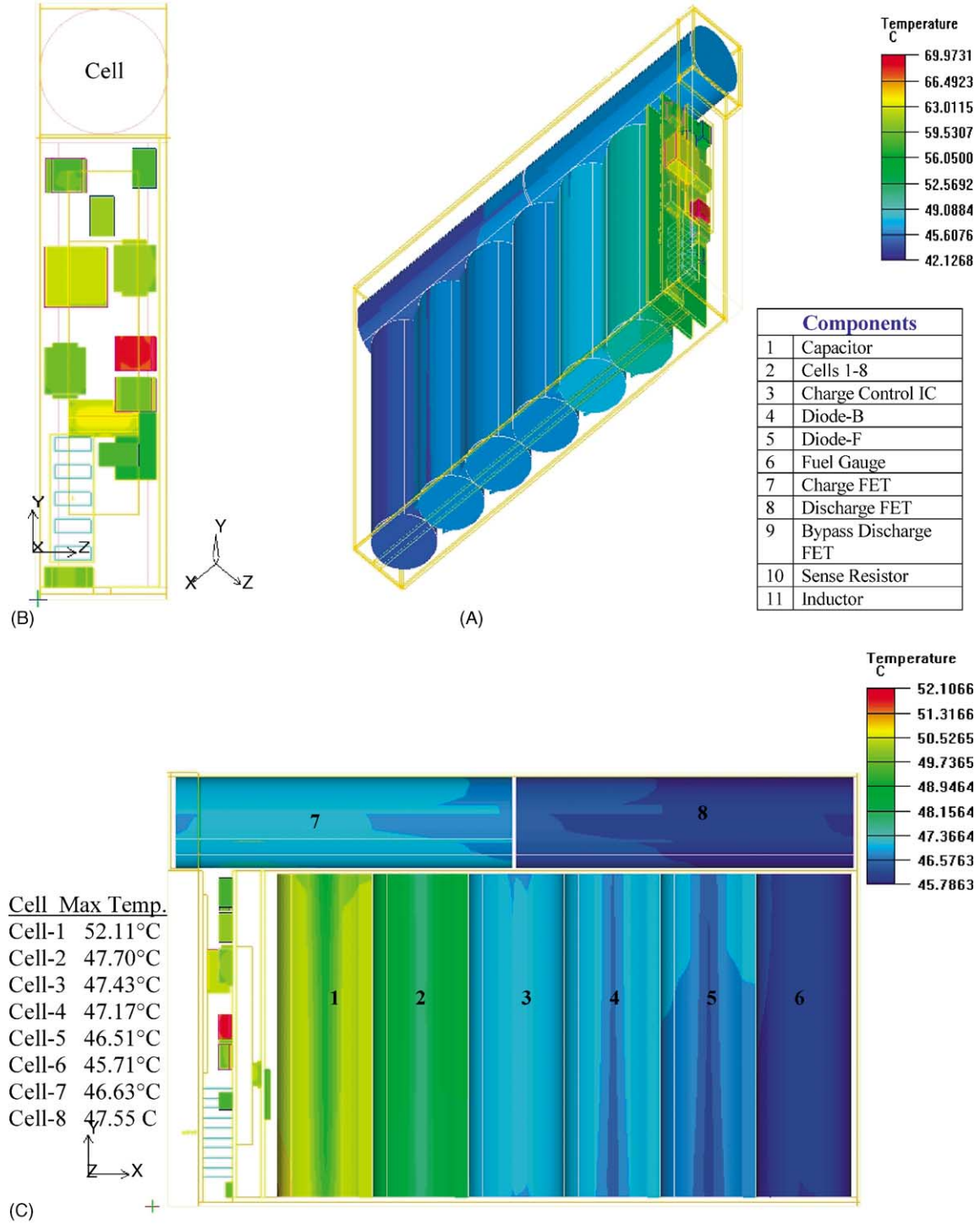

Fig. 4. (A) Global thermal profiles of the IBA2+ battery at the end of the charge state. (B) Global thermal profile of the power board in the IBA2+ battery. (C) Thermal profiles of the IBA2+ battery at the end of the charge state. Temperature profile is focused between 45 and 52 °C for higher resolution.

using an I^2R_{DSON} relation, where I (A) is current input and the R_{DSON} is the device resistance.

7. Allow conduction heat transfer inside and natural convection and conduction heat transfer outside of the battery-pack.

4. Results and discussion

Fig. 3A–C shows thermal profile of the interior of the battery-pack at the end of the discharge step when the cells temperatures rise are at a maximum. In Fig. 3C, the temperature range 62–71 °C is selected for a clearer distinction of temperature rise/distribution among the cells. Note that the cells nearest to the electronics assemblies are hotter than cells further away from them. Table 2 gives maximum temperature rise values (measured versus simulated) for cells and the critical electronic components in the battery at the end of discharge and charge steps. The overall results showed the battery interior temperature during discharge is dominated by the heat dissipation from the cells and during charge by the heat from the control electronics. Other critical issues were the cells temperature increasing above 60 °C and the non-uniformity in their temperature distribution, especially among the cells closest to electronics operating at near 70 °C.

Accelerating rate calorimetry (ARC) studies show that the onset of thermo-chemical reactions for most current commercial 18650 Li-ion cells, at fully charge state, start near 55 °C and for some cells at temperature as low as 47 °C. Storage of the same 18650 cells for 1 week at temperatures between 40 and 70 °C leads to permanent capacity loss of about 2–10%, depending on the cell type and temperature range. The most chemically stable Li-ion cells lose up to 27% of their initial capacity when stored at 60 °C (fully charged) and cycled once every 24 h for 20 days. This capacity fading reduced to ∼12% with temperature reduced from 60 to 55 °C. These results suggest that temperature distribution of 50–70 °C among the cells in laptop batteries could lead to some levels of capacity fading that can cause imbalance in cells performance and ultimately battery capacity fading. This issue becomes even more critical in cases of batteries used for running laptop computers with increasing processor speed (e.g. Pentium IV) that tend to generate more heat. For example, a 1-MHz processor generates ∼15 W heat, and this heat generation increases to about ∼27–30 W for the 2-MHz processor.

Fig. 4A–C shows thermal profiles of the interior of the battery at the end of the charge step when temperature rise of the charge control electronics are at a maximum. In Fig. 4C, the temperature range of 45–69 °C is selected for a clearer distinction of temperature rise/distribution among the cells in the battery-pack. Note that the cells nearest to the electronics assemblies are hotter than that those further away from them. However, the overall temperature of the cells remains below of 60 °C, but the internal temperature of the charge control-IC reaches 67 °C which is close to the upper critical temperature limit of the device. Some design changes mitigated this issue.

5. Conclusion

In this article, we have demonstrated the importance of thermal modeling and the accuracy of the selected methodology for computer battery-pack thermal management [6]. Thermal modeling facilitated electronics design with minimum possible power dissipation and clarified interactions effects of heat generation among electronics and cells during charge/discharge.

Acknowledgements

The authors would like to thanks Jason Howard from Motorola ESG Energy Technology Group and Jauhari Ghafar and K.H. Sim from Motorola Penang ESG Research and Development for providing us with details needed for understanding Li-ion battery thermal management issues and the opportunity to perform these simulation.

References

[1] S. Al Hallaj, J. Perkash, J.R. Selman, J. Power Sources 78 (2000) 186.
[2] M. Kramer, D. Karasek (Motorola PCS), Using CFD to characterize thermal performance of cellular products, in: Proceedings of the Hermes Symposium, Ft. Lauderdale, FL, 1999.
[3] Bert A. Zahn, Bench mark study of Ice-Pak vs. Flowtherm, in: Proceedings of the Inter Society Conference on Thermal Phenomena (IEEE/0-7803), 1998, p. 322.
[4] J.E. Greabner, Thermal Conductivity of Printed Wiring Board, Bell Lab Report, 1995.
[5] H. Maleki, S. Al-Hallaj, J.R. Selman, J. Electrochem. 146 (1999) 947.
[6] H. Maleki, Thermal modeling on computer battery, Portable Design Mag., December 2002 issue.